Biochemical and Biophysical Research Communications 516 (2019) 806–811

Contents lists available at ScienceDirect

Biochemical and Biophysical Research Communications

journal homepage: www.elsevier.com/locate/ybbrc

Nuclear aconitase antagonizes heterochromatic silencing by interfering with Chp1 binding to DNA

Soo-Jin Jung [a, 1], Yoonjung Choi [b, 1], Daeyoup Lee [b, *], Jung-Hye Roe [a, **]

[a] School of Biological Sciences, Institute of Microbiology, Seoul National University, Seoul, 151-742, South Korea
[b] Department of Biological Sciences, Korea Advanced Institute of Science and Technology, Daejeon, 34141, Republic of Korea

ARTICLE INFO

Article history:
Received 11 June 2019
Accepted 15 June 2019
Available online 27 June 2019

Keywords:
Aconitase
Chp1
Heterochromatin
RNAi-independent gene silencing
Anti-silencing factor

ABSTRACT

In *Schizosaccharomyces pombe*, there are two aconitases, Aco1 and Aco2, involved in the Krebs cycle in mitochondria. Interestingly, Aco2 is localized to nucleus as well. Here, we investigated the nuclear role of Aco2 by deleting its nuclear localization signal. The *aco2ΔNLS* mutation suppressed the gene-silencing defects of RNAi mutants at the centromere, where heterochromatin formation depends on RNAi pathway. In *Δago1*, the *aco2ΔNLS* mutation restored heterochromatin through elevating Chp1 binding. Aco2 physically interacted with Chp1 via the N-terminal chromodomain that binds to methylated histone H3K9. In the sub-telomeric region, where heterochromatin forms independent of RNAi pathway, the single *aco2ΔNLS* mutation caused extra gene silencing via elevating Chp1 binding, without increasing histone methylation. The anti-silencing effect did not require the catalytic function of aconitase. Taken together, Aco2 functions as an epigenetic regulator of gene expression, through associating with chromodomain of Chp1 to maintain heterochromatin.

© 2019 The Authors. Published by Elsevier Inc. This is an open access article under the CC BY-NC-ND license (http://creativecommons.org/licenses/by-nc-nd/4.0/).

1. Introduction

Aconitase functions as an enzyme in the Krebs cycle in bacteria and mitochondria. It also serves additional roles as a nucleic acid-binding protein. In mammals, cytosolic aconitase (IRP1) regulates iron homeostasis through its RNA binding activity [1,2]. In bacteria, aconitase binding to regulatory regions of RNA has been reported [3,4]. In *Saccharomyces cerevisiae*, Aco1p binds DNA and stabilizes mitochondrial DNA as a component of the mitochondrial nucleoid [5]. The presence of non-mitochondrial aconitase has been reported in the cytosol of *S. cerevisiae* [6] and in the nucleus of *Schizosaccharomyces pombe* [7,8].

Recently, there has been growing evidence that metabolic enzymes are linked to chromatin regulation in the nucleus through moonlighting non-canonical functions [9]. For example, pyruvate kinase 1, a key cytoplasmic enzyme in glycolysis, modifies chromatin by phosphorylating histone H3 in human [10] and in *S. cerevisiae* [11]. In contrast to cytoplasmic glycolytic enzymes, all of which are also found in the nucleus, a subset of mitochondrial TCA cycle enzymes are known to be present in the nucleus of specific cells [9,12]. In these cases, epigenetic regulation is primarily achieved by metabolites, such as fumarate and alpha-ketoglutarate, which can modulate the activity of histone and DNA demethylases. A link between aconitase and RNAi-mediated gene silencing has been suggested in *Caenorhabditis elegans*, where a genome-wide screening identified an aconitase gene (*aco2*) along with genes involved in known RNAi machinery components and heterochromatin formation [13]. How aconitase is related with gene silencing is not understood.

In fission yeast (*S. pombe*), heterochromatin is formed by both RNAi-dependent and RNAi-independent pathways [14,15]. Among the three constitutively heterochromatic loci (the centromere, mating type locus, and telomere), the centromere depends most heavily on the RNAi pathway to form heterochromatin. The RNA-induced transcriptional silencing (RITS) complex composed of Ago1, Chp1, and Tas3 is recruited to the nascent RNA via the Ago1-associated single-stranded siRNA [16]. The RITS complex associates with the chromatin via Chp1, an HP1 protein, that binds to the methylated Lys-9 residue of histone H3 (H3K9me) [16]. The RITS complex then recruits Clr4–Rik1–Cul4 (CLRC), of which Clr4 is the

* Corresponding author. Department of Biological Sciences, Korea Advanced Institute of Science and Technology, 291 Daehak-ro, Yuseong-gu, Daejeon, 34141, Republic of Korea.
** Corresponding author. School of Biological Sciences, Seoul National University, Seoul, 08826, South Korea.
E-mail addresses: daeyoup@kaist.ac.kr (D. Lee), jhroe@snu.ac.kr (J.-H. Roe).
[1] both authors contributed equally to this work.

https://doi.org/10.1016/j.bbrc.2019.06.090
0006-291X/© 2019 The Authors. Published by Elsevier Inc. This is an open access article under the CC BY-NC-ND license (http://creativecommons.org/licenses/by-nc-nd/4.0/).

methyltransferase that methylates H3K9, thus reinforcing heterochromatin formation [17]. Beyond the centromere, Chp1 associates with non-centromeric heterochromatin in an Ago1-independent manner [18]. At the telomere, Chp1-Tas3 platform regulates gene expression in an Ago1-independent pathway. It has been reported that the PIN domain of Chp1, which resides near C-terminus, post-transcriptionally silences the *tlh1+* transcripts [19].

Previously we demonstrated that Aco2 is localized in the mitochondria and in the nucleus, owing to the N-terminal mitochondrial targeting sequence and the C-terminal nuclear localization signal (NLS) [8]. Based on this observation and a clue from a *C. elegans* study to associate aconitase with RNAi-mediated gene silencing [13], we investigated the role of nuclear Aco2 in heterochromatin-associated gene silencing.

2. Materials and methods

2.1. Yeast strains

All the deletions and taggings were done through PCR-based gene targeting strategies [20]. Detailed method for constructing Aco2 mutants was shown in Supplementary information.

2.2. Chromatin immuno-precipitation (ChIP)

ChIP analysis was performed as previously described [21] with some modifications. The cell lysate was sonicated six times (20s on, 180s off) using an ultrasonicator with a microtip at 35% of maximum amplitude. The input (in whole cell extracts) and immunoprecipitated DNAs were amplified by qRT-PCR using the Stratagene MX300P QPCR system (Agilent Technologies) with analysis software MXpro (Agilent Technologies).

2.3. Information of Swi6 antibody

The polyclonal antibodies against Swi6 were raised in-house from rabbits as previously described [22].

2.4. ChIP-seq

Following immuno-precipitation, de-crosslinked DNAs were subjected to library construction for sequencing, using a NEXTflex™ Illumina ChIP-Seq Library Prep kit (BIOO) according to the manufacturer's protocol. The sequenced reads were aligned to the *S. pombe* genome (ASM294v2) by using NovoAlign (Novocraft technologies). BigWig files were generated using DeepTools [23].

2.5. RNA-seq

For library construction, mRNAs were purified using an NEBNext® Poly(A) mRNA Magnetic Isolation Module, and were subjected to library preparation using a NEXTflex™ Rapid Directional mRNA-Seq kit (BIOO) according to the manufacturer's instructions. The RNA library was sequenced on a HiSeq2500 using the single-end method (50-bp reads) and the reads were aligned to the *S. pombe* genome (ASM294v2) using the STAR aligner [24]. The alignment process produced BAM files, which were converted to bigWig files using SAMtools [25].

2.6. Small RNA northern blot analysis

Northern blot analysis of centromeric small RNAs was done as described previously [26]. For *dg/dh* siRNA detection, a mixture of IK8, IK9 and IK10 oligonucleotides (Table S3) was used. For loading control, snRNA58 was analyzed in parallel. Oligonucleotide probes were labeled at 5' ends with [γ-^{32}P]-ATP and T4 polynucleotide kinase. Autoradiography was analyzed by PhosphorImager (BAS-5000) and Multi Gauge (Fuji) Program.

2.7. Complementation of the aco2ΔN phenotype with aco2 variants

All strains used in the complementation assay were obtained by integrating different forms of the aco2 gene to the leu1 site in the *aco2ΔN* mutant. The wild type *aco2+* gene, the aconitase domain with its mitochondrial target sequence (1–25 aa; MTS-AD), the aconitase domain linked with the NLS from SV40 T antigen (NLS-AD), or the ribosomal protein domain with the embedded NLS (884–890 aa; RD) were cloned in pJK148 vector (addgene) [27]. To generate NLS-AD, the primer pair Aco2-NLS-F(NdeI) and Aco2-AD-R(BamHI) was used for PCR. After restriction digestion with *TthIII*, linearlized DNA was transformed into the *aco2ΔN* strain. A control strain JH42 was made by transforming linearlized pJK148 vector into ED665 cell.

2.8. Data deposition

The genome-wide datasets reported in this paper have been deposited in the Gene Expression Omnibus (GEO) repository under the accession No. GSE101804.

3. Results

3.1. Depleting nuclear Aco2 suppresses the gene-silencing defect of RNAi mutants in the centromeric region

In order to understand the function of Aco2 in the nucleus, we examined the phenotype of NLS-deleted *aco2* (*aco2ΔN*) mutant that fails to produce nuclear-localized Aco2 (Fig. 1A) [8]. To examine whether nuclear Aco2 is associated with RNAi-mediated gene silencing, we monitored gene expression in the centromeric region. Transcripts from the pericentromeric repeat region (*dg/dh*) were measured by quantitative real-time PCR (qRT-PCR) in the *aco2ΔN* mutant, as well as in RNAi mutants defective in centromeric heterochromatin formation. The *aco2ΔN* mutant by itself did not show any prominent effect on centromeric RNA transcription. However, when combined with mutations in RNAi pathway genes encoding Argonaute (*Δago1*) or Dicer (*Δdcr1*) that showed prominent gene-silencing defects, the *aco2ΔN* mutant suppressed the phenotype of both *Δago1* and *Δdcr1* mutants (Fig. 1B).

To gain further insight into how *aco2ΔN* mutant achieved gene silencing, we examined the extent of H3K9 methylation and recruitment of RNA polymerase II (RNAPII) and Swi6, an HP1 protein, in the pericentromeric region. We performed chromatin immunoprecipitation (ChIP) combined with high-throughput sequencing (ChIP-seq) using anti-H3K9me2 antibody. As shown in Fig. 1C, the level of H3K9me2 was highly enriched at the centromeric region in the wild type, while *Δago1* cells showed a significant decrease in the level of H3K9me2 in the centromeric repeat region. Consistent with the decreased transcripts from *dg/dh* repeats, H3K9me2 levels were higher in the *aco2ΔNΔago1* double mutants than in *Δago1* mutant, indicating RNAi-independent restoration of heterochromatin. The H3K9me2 ChIP-seq result was confirmed by conventional ChIP-qPCR of the repeat (*dg/dh*) region (Fig. S1A and B). Similarly, the *aco2ΔN* mutant also restored the H3K9me2 levels in the *Δdcr1* mutant, as judged by ChIP-qPCR analysis (Fig. S1C).

We then examined the level of RNAPII binding to the pericentromeric region. ChIP with antibody against RNAPII revealed that the *aco2ΔN* mutation significantly reduced the RNAPII binding that was highly enhanced in the *Δago1* mutant (Fig. 1D). This indicates

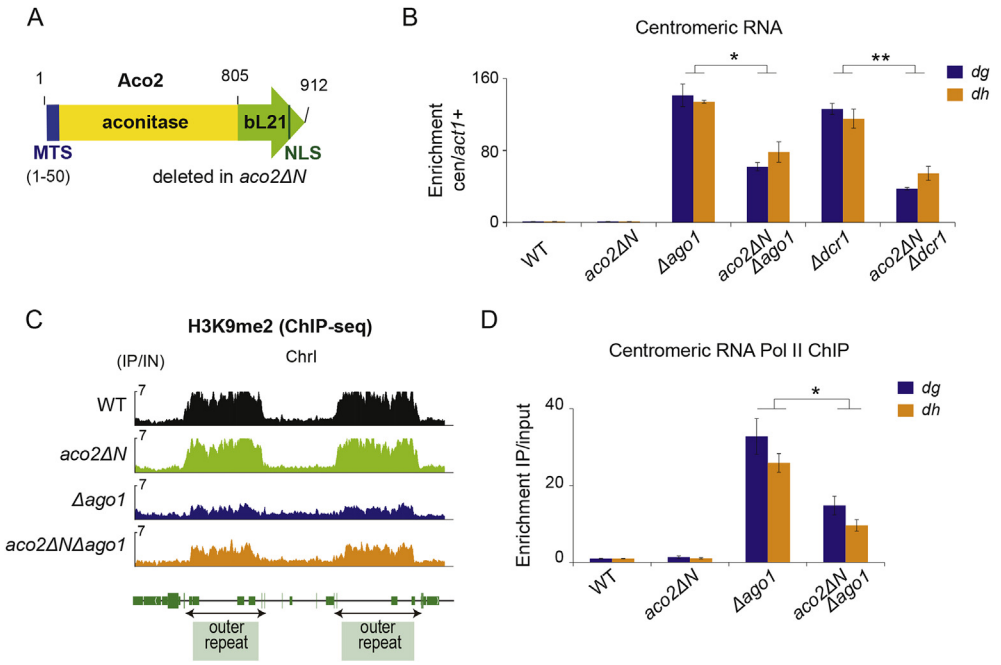

Fig. 1. The *aco2ΔN* mutation restores functional heterochromatin at centromeres in RNAi-deficient cells. (A) Domain structure of Aco2 with sub-cellular targeting signals. The *aco2ΔN* mutation deleted the NLS sequence (KHKRRHRH), resulting in the mutant protein to be localized exclusively in mitochondria [8]. (B) The level of centromeric *dg/dh* RNAs in *aco2ΔN* and RNAi mutants. Relative enrichment (centromeric RNA/*act1+*) values were plotted for each sample. (C) H3K9me2 ChIP-seq profile at the centromeric region of chromosome I in various strains, as shown by IGV genome browser. Each ChIP signal was normalized to input signal. (D) RNA polymerase II binding monitored by ChIP-qPCR. For each strain, qRT-PCR and ChIP-qPCR analyses were done with three independent samples. * and ** denote P-values less than 0.05 and 0.01, respectively, by Student's t-tests.

that the decrease in RNA transcripts in the centromeric region is primarily due to transcriptional silencing rather than enhanced RNA degradation. We also examined the effect of *aco2ΔN* mutant on Swi6 binding to the pericentromeric region by Swi6 ChIP-qPCR analysis. Introduction of *aco2ΔN* mutant to the *Δago1* mutant restored Swi6 binding to the level of the wild type (Fig. S1D). This coincides with the elevation of H3K9me2 by *aco2ΔN* mutant in *Δago1* mutant.

To verify the RNAi-independent formation of heterochromatin by aco2*ΔN* in the *Δago1* background, we examined small RNAs produced from the centromeric repeats by northern blot analysis (Fig. S1E). In the *Δago1* mutant, *dg/dh* siRNAs were not detected by northern analysis, which was consistent with previous observations [28]. Introduction of the *aco2ΔN* did not restore the level of siRNAs in the *Δago1* mutant. Therefore, the suppression of the RNAi mutant phenotype by *aco2ΔN* mutant occurred independently of siRNA formation.

3.2. Heterochromatin-associated activity of nuclear Aco2 depends on Chp1

Since the silencing defect caused by depletion of Ago1 was rescued by the *aco2ΔN*, we also checked whether Chp1, another component of the RITS complex, could be suppressed by the loss of nuclear Aco2. In contrast to its effect on *Δago1* and *Δdcr1* mutants, *aco2ΔN* mutant did not appear to suppress the silencing defects of *Δchp1* mutant when centromeric *dg/dh* transcripts were monitored (qRT-PCR; Fig. 2A). RNAPII binding to its corresponding region was not affected by the *aco2ΔN*, as analyzed by ChIP (Fig. 2B). This indicates that the ability of nuclear Aco2 to modulate heterochromatin formation in an RNAi-independent manner depends on Chp1. To examine this hypothesis, we monitored the level of Chp1 enrichment in the centromeric region by Chp1 ChIP analysis. The results in Fig. 2C demonstrated that the Chp1 binding to the centromeric region was reduced in the absence of Ago1, but surprisingly in the *aco2ΔNΔago1* double mutants, the Chp1 binding was restored to the level of the wild type. We also investigated the effect of Tas3 on the heterochromatin modulation by Aco2, since Chp1 interacts with Tas3 tightly and make multifunctional platform [19]. By monitoring H3K9me2 enrichment at the centromeric *dg/dh* region by ChIP-qPCR, we found that the restoration of heterochromatin by *aco2ΔN* in the *Δago1* mutant background did not occur when *Δtas3* was additionally introduced (Fig. S2). The *aco2ΔN* also did not restore the decreased H3K9me2 level in the *Δtas3* mutant. This observation indicated that Chp1 worked together with Tas3 in increasing H3K9me2 in the *aco2ΔNΔago1* mutant.

3.3. Aco2 interacts with Chp1 through the chromodomain

We then examined whether Aco2 physically interacts with Chp1 by co-immunoprecipitation (co-IP) experiments. For this purpose, *S. pombe* strains expressing Chp1-MYC with or without Aco2-FLAG were constructed. Using anti-FLAG affinity beads, Aco2-FLAG-associated proteins in cell lysates were precipitated and analyzed by Western blot. Fig. 3A demonstrates that Chp1 specifically interacted with Aco2. To dissect the domain of Chp1 that interacts with Aco2, a GST pull-down assay was performed. Five different fragments of Chp1, N-terminally tagged with GST, were expressed and purified from *E. coli*. Each Chp1 fragment was incubated with *S. pombe* cell extracts containing Aco2-FLAG, followed by precipitation with glutathione-coated beads. Proteins in the supernatant (S) and the pulled-down (B) fractions were analyzed for Aco2 by Western blot with anti-FLAG antibody. The results in Fig. 3B

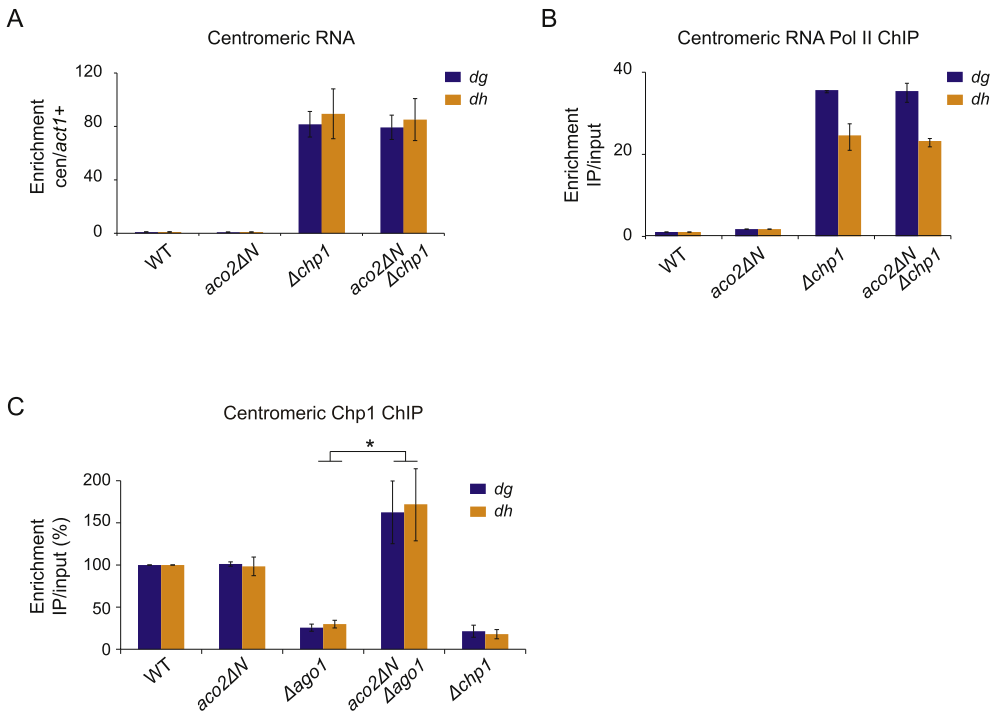

Fig. 2. Dependence of Aco2 association with centromeric chromatin on Chp1. (A) The centromeric *dg/dh* RNAs were monitored by qRT-PCR in the wild type, *aco2ΔN*, *Δchp1*, and *aco2ΔNΔchp1*. Relative enrichment (centromeric RNA/*act1*+) values from three independent experiments were plotted. (B) Levels of Pol II binding to the centromeric repeat region were monitored by ChIP-qPCR. (C) ChIP analysis of Chp1 binding to the centromeric region in the wild type, *aco2ΔN*, *Δago1*, *aco2ΔNΔago1*, and *Δchp1* mutants. Average values from three independent experiments were presented with standard deviations. * denote a P-value ≤ 0.05 by Student's t-tests.

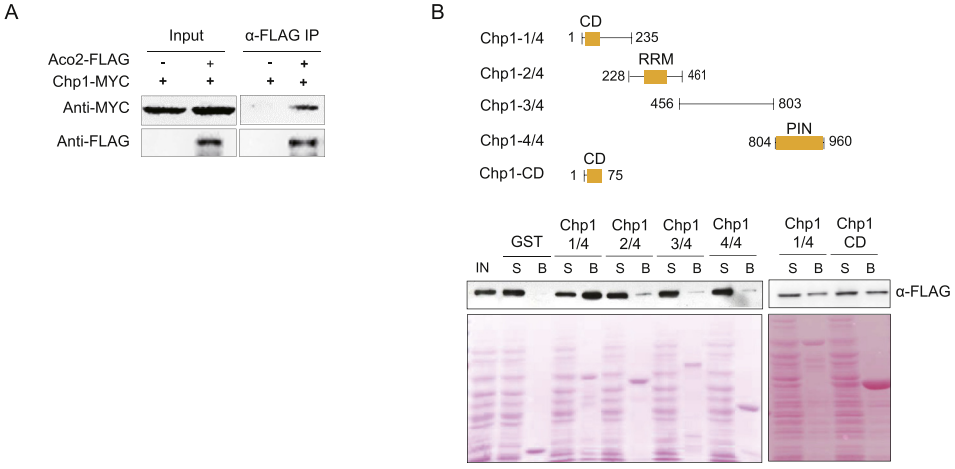

Fig. 3. Physical interaction between Aco2 and Chp1. (A) Co-Immunoprecipitation of Aco2-FLAG and Chp1-MYC. Extracts from cells expressing Chp1-MYC alone or with Aco2-FLAG were analyzed by Western blot before (input) or after immunoprecipitation with anti-FLAG antibody. (B) GST pull-down analysis of interactions between Aco2 and GST-fused fragments of Chp1. Five different portions of Chp1 were fused to GST on a pET15b plasmid; Chp1-1/4 (1–235 aa), Chp1-2/4 (228–461), Chp1-3/4 (456–803), Chp1-4/4 (804–960), and Chp1-CD (chromodomain; 1–75). Each recombinant protein was incubated with cell-free extracts of *S. pombe* cells expressing Aco2-FLAG. Following GST-pull down with glutathione-coated resin, the presence of Aco2 in the supernatant (S) and bound (B) fractions was examined by Western blot analysis with anti-FLAG antibody. The Ponceau-stained protein gel was presented below.

showed that the first quarter of Chp1 (1/4, 1–235 aa), containing the chromodomain, preferentially interacted with Aco2-FLAG, whereas the other fragments (2/4, 3/4, and 4/4) bound Aco2 only marginally. These results demonstrate that Aco2 can bind Chp1 through the N-terminal region. We further trimmed down Chp1 and found that the N-terminal 75 aa that encompasses the chromodomain (20–75 aa) interacted with Aco2 (Fig. 3B). Since the chromodomain of Chp1 is known to interact with H3K9me and RNA [18,19,29], it can be postulated that Aco2 may interfere with Chp1 binding to the methylated histones.

3.4. *The aco2ΔN single mutation causes gene silencing at subtelomeric loci via recruiting Chp1*

To further investigate the function of nuclear Aco2, we examined by transcriptome analysis in *aco2ΔN* mutant whether the

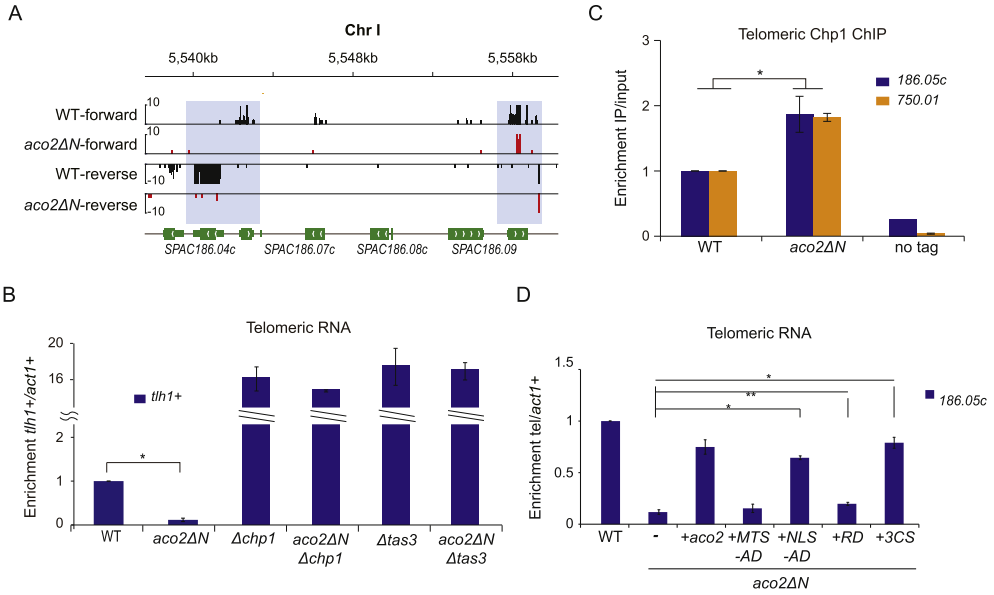

Fig. 4. The *aco2ΔN* single mutation leads to gene silencing at telomeric loci. (A) IGV genome browser snapshots of a telomeric region (right end of chromosome I), showing RNA occupancy in *aco2ΔN* in comparison with the wild type. The forward- and reverse-strand read profiles from RNA-seq analysis of the wild-type and *aco2ΔN* cells were shown with the boxed highlights where *aco2ΔN* mutation reduced gene expression. (B) Relative *tlh1*$^+$ gene expression (*tlh1*$^+$/*act1*$^+$) values were plotted for each strain. (C) ChIP-qPCR for Chp1 binding to the telomeric loci (SPAC186.05c and SPAC 750.01) in the wild type and *aco2ΔN* mutant. The graphs represent data averaged from three independent experiments, with the standard deviations. * indicates a P-value < 0.05 by Student's t-tests. (D) Expression of the SPAC186.05c gene in the telomeric region was examined in various strains. The *aco2ΔN* mutant was complemented with the wild type *aco2*$^+$ gene, or modified genes encoding an aconitase domain with mitochondrial targeting sequence (MTS-AD), nuclear localization signal (NLS-AD), or the ribosomal protein domain with embedded NLS (RD), or Aco2 with Cys to Ser substitution mutations of three conserved cysteines (3CS). Following qRT-PCR, the relative enrichment (SPAC186.05c/*act1*+) values were obtained from three independent experiments. The average values with standard deviations were presented. * and ** indicate P-values less than 0.05 and 0.0001, respectively, by Student's t-tests.

aco2ΔN mutation affects gene expression. Notably, we found that genes near the telomere were significantly silenced in the *aco2ΔN* mutant, as represented by the right telomeric region of chromosome I in Fig. 4A. Similar silencing effect of the *aco2ΔN* was observed in all the other telomeric regions except chromosome III (Fig. S3). We examined by conventional qRT-PCR transcripts from the *tlh1*$^+$ locus in the subtelomeric region, encoding a telomere-linked helicase and known to be regulated by Chp1-Tas3 platform in RNAi-independent manner [19]. The result confirmed that the *aco2ΔN* by itself caused significant gene silencing by about 10-fold in the *tlh1*$^+$ locus (Fig. 4B). In the absence of Chp1 or Tas3, *tlh1*$^+$ expression increased by more than 16-fold relative to the wild-type level, and the *aco2ΔN* did not suppress the silencing-defective phenotype of the *Δchp1* or *Δtas3* mutants (Fig. 4B). This implies that like the centromeric region, Aco2 could prevent excessive gene silencing in the telomeric region, caused by Chp1 and Tas3 in an RNAi-independent manner.

We then examined whether the *aco2ΔN* caused changes in the level of Chp1 binding to the telomeric region. The ChIP experiment with anti-FLAG antibody to detect Chp1-FLAG binding to telomeric loci (SPAC186.05c and SPAC 750.01) indicated that the *aco2ΔN* caused significant increase in the binding of Chp1 to the telomeric loci (Fig. 4C). However, the *aco2ΔN* showed no change in H3K9me2 level (Fig. S3A). Collectively, these observations indicate that Aco2 exerts its anti-silencing effect in the telomeric region via interfering with Chp1 binding.

3.5. The aconitase domain of Aco2 exerts the anti-silencing effect without the need for the catalytic activity

Aco2 consists of an aconitase domain and a mitochondrial ribosomal protein domain (bL21) that harbors a NLS sequence (Fig. 1A) [8]. In order to delineate the domain that is responsible for the nuclear anti-silencing function, the effect of each domain in complementing the phenotype of the *aco2ΔN* mutant was examined. Transcripts from a telomeric locus (SPAC186.05c) were monitored by qRT-PCR. The low-level expression of the telomeric locus in the *aco2ΔN* mutant was restored to about 70% of the wild type strain by introducing the wild type *aco2*$^+$ gene to the chromosomal *leu1* site (Fig. 4D). The aconitase domain with its mitochondrial targeting sequence (MTS-AD) did not complement the mutant phenotype, whereas the aconitase domain linked with the NLS from SV40 T antigen (NLS-AD) restored the telomeric gene expression to the level of the wild type *aco2*$^+$ complementation. The ribosomal bL21 domain with the embedded NLS (RD) did not restore the telomeric gene expression. These results clearly demonstrated that the anti-silencing role of Aco2 relies on the aconitase domain. We then examined whether the catalytic function of aconitase is needed, by introducing a mutant Aco2 whose conserved three cysteines required for catalytic activity were replaced with serines (3CS). The non-catalytic mutant Aco2 fully restored the telomeric gene expression to the level achieved by the wild type *aco2*$^+$ complementation. This indicates that the chromatin-modulation by Aco2 does not require its enzymatic function, ruling out the possibility of indirect contribution of Aco2 via changing metabolites.

4. Discussion

In this study, we showed that Aco2, a fusion protein of aconitase and mitochondrial ribosomal protein bL21 in *S. pombe*, modulates gene expression in the nucleus by directly interacting with Chp1 and interfering with its gene-silencing function. In the centromeric region where heterochromatic gene silencing occurs largely in RNAi-dependent pathway, the *aco2ΔN* suppressed the gene-silencing defects of the RNAi mutants by restoring

heterochromatin formation. Chromatin modulation by Aco2 at the centromere depended on Chp1 and Tas3, components of the Ago1-containing RITS complex, which has a pivotal role in siRNA production and recruitment of the H3K9 methyltransferase Clr4 [28].

It has been demonstrated that Chp1 and Tas3, two subunits of the RITS complex, localize to non-centromeric regions and induce RNAi-independent gene silencing [19]. The mechanism and regulation of RNAi-independent heterochromatin formation in non-centromeric regions are not well understood. The pronounced effect of Aco2 in the telomeric region reveals a pathway by which Chp1 action can be regulated apart from the RNAi pathway. In the sub-telomeric loci, the *aco2ΔN* mutation caused an increased Chp1 binding and extra gene silencing, without changing heterochromatin or RNAPII binding. Chp1 is known to regulate the *tlh1*$^{+}$ gene expression through post-transcriptional gene silencing (PTGS) via the PIN domain [19]. Therefore, it is likely that Aco2 modulates PTGS by interfering with Chp1 action, which depends on Tas3 as well. Based on these observations, we postulate that Aco2 serves as a fine tuner of gene expression by suppressing high loading of Chp1 in RNAi-independent heterochromatic region.

This novel nuclear function of Aco2 registers this protein as one of the most versatile proteins across bacterial and eukaryotic domains. A genome-wide screening study in *S. cerevisiae* discovered an aconitase gene (*ACO2*; yJL200C) involved in telomeric fold-back structures [29]. Therefore, it is likely that the role of aconitase as a chromatin-modulator to control gene expression is shared across different biological systems. Furthermore, it is worth noting that the conserved cysteines critical for the catalytic function are not required for the nuclear role of Aco2. This feature not only excludes the possibility that Aco2 indirectly regulates chromatin by changing metabolites as an enzyme. The nature as well as the mechanism of crosstalk between physiological status and nuclear epigenetic regulation via Aco2 that shuttles between mitochondrial matrix and nuclear chromosome is an intriguing question to solve in the near future.

Acknowledgements

This work was supported by grants from the National Research Foundation of Korea (NRF) to DL (2018M3C9A6065070) and JHR (2017R1A2A1A05000735). SJ Jung was supported by the BK21-Plus fellowship for graduate students for Biological Sciences at SNU.

Appendix A. Supplementary data

Supplementary data to this article can be found online at https://doi.org/10.1016/j.bbrc.2019.06.090.

Transparency document

Transparency document related to this article can be found online at https://doi.org/10.1016/j.bbrc.2019.06.090

References

[1] H. Beinert, M.C. Kennedy, Aconitase, a two-faced protein: enzyme and iron regulatory factor, FASEB J. 7 (1993) 1442–1449.
[2] R.D. Klausner, T.A. Rouault, A double life: cytosolic aconitase as a regulatory RNA binding protein, Mol. Biol. Cell 4 (1993) 1–5.
[3] C. Alen, A.L. Sonenshein, Bacillus subtilis aconitase is an RNA-binding protein, Proc. Natl. Acad. Sci. U.S.A. 96 (1999) 10412–10417.
[4] Y. Tang, J.R. Guest, Direct evidence for mRNA binding and post-transcriptional regulation by Escherichia coli aconitases, Microbiology 145 (Pt 11) (1999) 3069–3079.
[5] X.J. Chen, X. Wang, B.A. Kaufman, R.A. Butow, Aconitase couples metabolic regulation to mitochondrial DNA maintenance, Science 307 (2005) 714–717.
[6] N. Regev-Rudzki, S. Karniely, N.N. Ben-Haim, O. Pines, Yeast aconitase in two locations and two metabolic pathways: seeing small amounts is believing, Mol. Biol. Cell 16 (2005) 4163–4171.
[7] A.M. Duchene, P. Giege, Dual localized mitochondrial and nuclear proteins as gene expression regulators in plants? Front. Plant Sci. 3 (2012) 221.
[8] S.J. Jung, Y. Seo, K.C. Lee, D. Lee, J.H. Roe, Essential function of Aco2, a fusion protein of aconitase and mitochondrial ribosomal protein bL21, in mitochondrial translation in fission yeast, FEBS Lett. 589 (2015) 822–828.
[9] A.E. Boukouris, S.D. Zervopoulos, E.D. Michelakis, Metabolic enzymes moonlighting in the nucleus: metabolic regulation of gene transcription, Trends Biochem. Sci. 41 (2016) 712–730.
[10] W. Yang, Y. Xia, D. Hawke, X. Li, J. Liang, D. Xing, K. Aldape, T. Hunter, W.K. Alfred Yung, Z. Lu, PKM2 phosphorylates histone H3 and promotes gene transcription and tumorigenesis, Cell 150 (2012) 685–696.
[11] S. Li, S.K. Swanson, M. Gogol, L. Florens, M.P. Washburn, J.L. Workman, T. Suganuma, Serine and SAM responsive complex SESAME regulates histone modification crosstalk by sensing cellular metabolism, Mol. Cell 60 (2015) 408–421.
[12] R. Nagaraj, M.S. Sharpley, F. Chi, D. Braas, Y. Zhou, R. Kim, A.T. Clark, U. Banerjee, Nuclear localization of mitochondrial TCA cycle enzymes as a critical step in mammalian zygotic genome activation, Cell 168 (2017) 210–223 e211.
[13] J.K. Kim, H.W. Gabel, R.S. Kamath, M. Tewari, A. Pasquinelli, J.F. Rual, S. Kennedy, M. Dybbs, N. Bertin, J.M. Kaplan, M. Vidal, G. Ruvkun, Functional genomic analysis of RNA interference in C. elegans, Science 308 (2005) 1164–1167.
[14] M. Buhler, W. Haas, S.P. Gygi, D. Moazed, RNAi-dependent and -independent RNA turnover mechanisms contribute to heterochromatic gene silencing, Cell 129 (2007) 707–721.
[15] R.C. Allshire, K. Ekwall, Epigenetic regulation of chromatin states in Schizosaccharomyces pombe, Cold Spring Harb. Perspect Biol. 7 (2015), a018770.
[16] M. Buhler, A. Verdel, D. Moazed, Tethering RITS to a nascent transcript initiates RNAi- and heterochromatin-dependent gene silencing, Cell 125 (2006) 873–886.
[17] K. Zhang, K. Mosch, W. Fischle, S.I. Grewal, Roles of the Clr4 methyltransferase complex in nucleation, spreading and maintenance of heterochromatin, Nat. Struct. Mol. Biol. 15 (2008) 381–388.
[18] V.J. Petrie, J.D. Wuitschick, C.D. Givens, A.M. Kosinski, J.F. Partridge, RNA interference (RNAi)-dependent and RNAi-independent association of the Chp1 chromodomain protein with distinct heterochromatic loci in fission yeast, Mol. Cell. Biol. 25 (2005) 2331–2346.
[19] T. Schalch, G. Job, S. Shanker, J.F. Partridge, L. Joshua-Tor, The Chp1-Tas3 core is a multifunctional platform critical for gene silencing by RITS, Nat. Struct. Mol. Biol. 18 (2011) 1351–1357.
[20] M.D. Krawchuk, W.P. Wahls, High-efficiency gene targeting in Schizosaccharomyces pombe using a modular, PCR-based approach with long tracts of flanking homology, Yeast 15 (1999) 1419–1427.
[21] S. Strahl-Bolsinger, A. Hecht, K. Luo, M. Grunstein, SIR2 and SIR4 interactions differ in core and extended telomeric heterochromatin in yeast, Genes Dev. 11 (1997) 83–93.
[22] S. Oh, K. Jeong, H. Kim, C.S. Kwon, D. Lee, A lysine-rich region in Dot1p is crucial for direct interaction with H2B ubiquitylation and high level methylation of H3K79, Biochem. Biophys. Res. Commun. 399 (2010) 512–517.
[23] F. Ramirez, F. Dundar, S. Diehl, B.A. Gruning, T. Manke, deepTools: a flexible platform for exploring deep-sequencing data, Nucleic Acids Res. 42 (2014) W187–W191.
[24] A. Dobin, C.A. Davis, F. Schlesinger, J. Drenkow, C. Zaleski, S. Jha, P. Batut, M. Chaisson, T.R. Gingeras, STAR: ultrafast universal RNA-seq aligner, Bioinformatics 29 (2013) 15–21.
[25] H. Li, R. Durbin, Fast and accurate short read alignment with Burrows-Wheeler transform, Bioinformatics 25 (2009) 1754–1760.
[26] E.H. Bayne, M. Portoso, A. Kagansky, I.C. Kos-Braun, T. Urano, K. Ekwall, F. Alves, J. Rappsilber, R.C. Allshire, Splicing factors facilitate RNAi-directed silencing in fission yeast, Science 322 (2008) 602–606.
[27] J.B. Keeney, J.D. Boeke, Efficient targeted integration at leu1-32 and ura4-294 in Schizosaccharomyces pombe, Genetics 136 (1994) 849–856.
[28] M. Halic, D. Moazed, Dicer-independent primal RNAs trigger RNAi and heterochromatin formation, Cell 140 (2010) 504–516.
[29] H. Poschke, M. Dees, M. Chang, S. Amberkar, L. Kaderali, R. Rothstein, B. Luke, Rif2 promotes a telomere fold-back structure through Rpd3L recruitment in budding yeast, PLoS Genet. 8 (2012) e1002960.